Proceedings of 8th International Conference on Mechanical Engineering and Renewable Energy 2025
10-12 December, 2025, Chattogram, BANGLADESH
SciEn Conference Series: Engineering Vol. 4, 2026, pp 567-572 https://doi.org/10.38032/scse.2026.4.253

Bio-inspired Wing Morphologies for Underwater Gliders: Reducing Wake Instabilities and Resonance Risk

Gazi Arman Hossain[1,2,*], *Md Absar Jahan*[1], *Nayem Zaman Saimoon*[1], *Md. Fhamid Hasan*[1], *Mahadi Hasan Masud*[1]

[1]Department of Mechanical Engineering, Rajshahi University of Engineering & Technology (RUET), Rajshahi, Bangladesh
[2]Department of Industrial Engineering, BGMEA University of Fashion & Technology, Dhaka, Bangladesh

ABSTRACT

This study investigates the structural response of underwater glider (UWG) wings with various profiles for minimising vortex-induced vibrations (VIVs) and enhancing operational stability. Three wing geometries, a conventional rectangular cross-section (RCS), a NACA 2412 airfoil, and a biomimetic profile inspired by the Green Sea Turtle (GST), were compared through transient computational fluid dynamics (CFD) and modal analysis. Vortex shedding frequencies (VSFs) were determined by Fast Fourier Transform (FFT) of unsteady lift coefficients and compared to natural frequencies corrected for added mass in underwater conditions. The result shows that the GST-inspired wing offers superior stiffness and reduced unsteady loading, while the NACA 2412 and the RCS profiles achieved efficient flow attachment but may be more susceptible to resonance due to closer alignment of VSFs and modal frequencies. Results show that the GST-inspired wing exhibits the largest gap between hydrodynamic and structural frequencies, with around 132.33 Hz difference between its VIV and wet-modal frequencies, compared with 28.14 Hz for the RCS and 108.99 Hz for the NACA 2412. Thus, the GST wing demonstrated sufficient difference between hydrodynamic and structural timescales, minimising resonance risk. These findings demonstrate that the baseline NACA 2412 airfoil and biomimetic-based wing designs are promising for vibration attenuation and increased UWG endurance.

Keywords: Underwater Glider Wing, Bio-inspired Modification, Computational Fluid Dynamics, Modal Analysis, Wake instability.

1. Introduction

Underwater gliders (UWGs) are autonomous vehicles designed for long-duration ocean exploration, operating efficiently by utilising buoyancy-driven propulsion instead of conventional propellers. Their ability to travel vast distances with minimal energy consumption makes them suitable tools for oceanographic research, environmental monitoring, and resource management [1]. The hydrodynamic efficiency of a UWG depends mainly on its wing, and as the hydrodynamic efficiency directly dictates its endurance and manoeuvrability, thus, studying the wings of UWGs is essential to enhance performance and extend mission capabilities [2]. The legacy UWG models, such as Slocum, Petrel, and Spray gliders, typically have simple flat-plate-like wings with finite thickness to generate the hydrodynamic forces required for gliding. When operating at a nonzero angle of attack (AoA), these wings experience significant flow separation as well as periodic vortex shedding (VS), leading to unsteady variations in lift and drag forces. Such fluctuating hydrodynamic loading can give rise to fluid-structure interaction (FSI) effects, often demonstrated as a sinusoidal force pattern on the wing. If the frequency of VS coincides with any of the natural frequencies of the wing, resonance may occur, amplifying structural vibrations. This resonance may lead to excessive oscillations, fatigue, and even structural failure, highlighting the importance of understanding and controlling FSI in UWG wing design. Wang *et al.* (2025) first shed light on this matter in their work by the numerical simulation as well as experimental study in sea trial, and demonstrated that the three-dimensional vibrations of the wing are primarily dominated by bending and torsional modes [3]. The observed correlation between pressure fluctuations in the surrounding fluid and the wing's structural modes confirms that these modal responses play a significant role in generating flow-excited noise. Their work has provided a validated framework for vibration prediction and suppression in UWG wing design as well as laid the groundwork for redesigning wing geometry to reduce hydrodynamic vibration, noise, and improve acoustic payload fidelity [3]. However, to the best knowledge of the authors of the current study, there has been no published study where the researchers have proposed any vibration mitigation strategy for the above-stated issue. Moreover, replacing the conventional flat-plate wings with baseline NACA profiles as well as biomimetic profiles can substantially improve the hydrodynamic performance of UWGs, as the flow characteristics around these profiles are far superior to the existing wing models, as those profiles can cause delayed flow separation and streamwise vortices [4–6]. Thus, these design considerations have the potential to result in less unsteady hydrodynamic loading, reduced vortex-induced vibrations (VIV), and improved structural stability during gliding, ultimately enhancing the endurance, manoeuvrability, and overall performance of UWGs. Thus, this study aims to investigate the hydrodynamic characteristics of UWG wings with alternative airfoil designs, including a baseline NACA airfoil and a bio-inspired profile, to reduce unsteady hydrodynamic loading and mitigate vibration-induced stresses on the wing. The study focuses on analysing vortex dynamics and modal responses to identify wing configurations that minimise structural vibrations, enhance stability, and thereby improve the endurance and overall performance of UWGs.

2. Research Methodology

The hydrodynamic loads on three different UWG wing geometries were investigated through CFD simulations. A steady-state CFD run was first performed to obtain an initial converged solution, followed by transient CFD simulations to capture the unsteady wake dynamics and extract the time history of the lift coefficient (C_L). Fast Fourier Transform (FFT) of the C_L time history as the input signal revealed the dominant excitation frequency associated with VS, which was compared against the natural frequencies of the wings obtained from modal analysis to assess the potential risk of resonance.

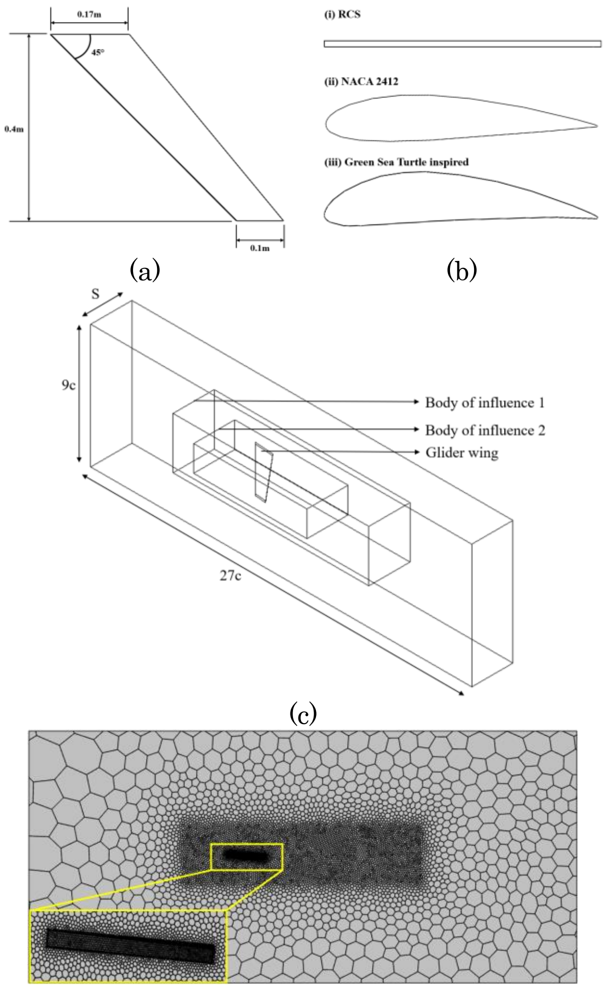

Fig. 1 (a) Dimension of Wing geometry (b) 3 different wing cross sections (c) Flow domain with dimension and body of influence (d) Mesh structure for the analysis

Fig. 1(a) shows the dimensions used for the UWG wings. Using the same chord and span length, sweep angle and taper ratio, three different wings were modelled in SolidWorks based on the profiles illustrated in Fig. 1(b). In this study, the reference UWG wing has a rectangular cross-section (RCS) profile with a thickness of 3 mm [3], and the other two wings were modelled based on a NACA2412 airfoil profile and a biomimetic profile inspired by the Green Sea Turtle (*Chelonia mydas*) wing [5, 6].

To perform the CFD, a 3D computational domain of 27c×9c×S was created in Ansys DesignModeler (illustrated in Fig. 1(c)). There are 2 stages of 'Body of Influence' within the computational domain. The element sizes of the "Body of Influence" 1 and 2 were 6.4×10^{-2} m, and 8×10^{-3} m. For the face sizing, the element size was 2×10^{-3} m. A total of 6 inflation layers was set, where the Y+ value was 1, and the thickness of the first layer was 3.5×10^{-5} m. The final mesh used has the following mesh quality parameters: maximum skewness and minimum orthogonal quality were 0.81 and 0.14. The k-*ω* model in the ANSYS Fluent software environment was then used to solve the 3D domain numerically. The numerical simulations were carried out using an inlet velocity of 0.5 m/s at 5° AoA, corresponding to a Reynolds number (*Re*) of 67.5×10^4. Table 1 presents the key overviews and boundary conditions utilised in this study.

Table 1 Key parameters for numerical simulation setup.

Parameter	Value/Type
Boundary conditions	Velocity inlet
	Pressure outlet
	Wall no-slip
Angle of attack	5°
Flow velocity	0.5 m/s
Reynolds number	$6.7\text{x}10^4$
Analysis type	Transient
Viscous model	k-ω (SST)

With the setup, a transient simulation of 1000 time steps (0.1s each) was run. The lift force time history was then extracted. The fluctuating lift force provides a direct measure of the unsteady hydrodynamic loading associated with VS. Consequently, the time history of the lift coefficient, C_L(t), is widely used to extract the dominant forcing frequency in flow-induced vibration studies [7–9]. To ensure statistical reliability, the first 15 seconds of the time history were then discarded, as they correspond to numerical startup effects rather than physical oscillations. Through FFT, a Power Spectral Density vs. frequency graph is plotted using Python coding. This gives the dominant vortex shedding frequency (VSF) caused by the unsteady wake interaction.

To assess the resonance risk of the wing, the natural frequency of the wing structure underwater environment is determined. Material for the wing was selected as carbon fibre, based on Wang *et al.* 2025, which has an elastic modulus of 291 GPa, Poisson's ratio of 0.3, and density of 1420 kg/m^3 [3]. In ANSYS Modal, the material was created, and a modal analysis was done on each wing geometry, keeping the root of the wing as a fixed support (as shown in Fig. 2). Meshing was done on the wing with a body size of 0.01m. After solving for total deformation, the frequencies for three different mode shapes were evaluated along with their corresponding deformation pattern.

In an underwater environment, the surrounding water contributes to added mass, which reduces the natural frequency of the structure and also provides hydrodynamic damping. Therefore, the dry natural frequencies obtained from modal analysis were corrected using an added-mass factor to estimate the wet natural frequencies, as given by the following equation [10–12],

$$f_{wet} = \frac{f_{dry}}{\sqrt{1 + \frac{m_{fluid}}{m_{structure}}}} \qquad (1)$$

The effective mass, $m_{structure}$, was extracted from the solution of ANSYS modal, and the added mass, m_{fluid}, was determined by the following equation [10]:

$$m_{fluid} = C_m \rho V \qquad (2)$$

Where, C_m is the added-mass coefficient, ρ is the fluid density, and V is the volume of displaced fluid.

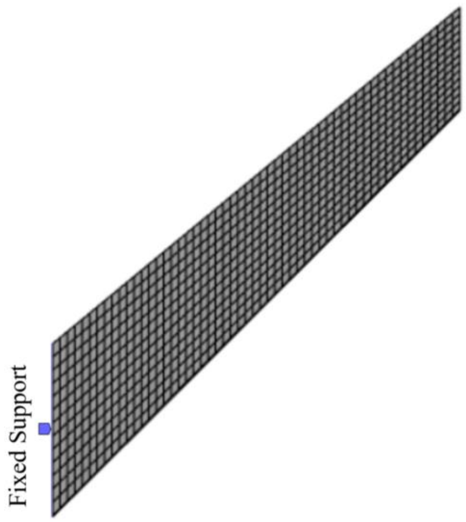

Fig. 2 Mesh on wing geometry with fixed support at the root.

3. Results and Discussion

Fig. 3 presents the modal analysis of the three wing geometries, which revealed distinct deformation patterns corresponding to the first three vibration modes. For all wing configurations, the first bending or torsional mode dominated the low-frequency response, while other modes mainly exhibited localised deformations. The baseline NACA 2412 and biomimetic Green Sea Turtle (GST)-inspired wing exhibited noticeably higher first-mode natural frequencies of 166.36 and 195.99 Hz compared to the RCS wing with only 31.04 Hz, indicating greater stiffness. The GST wing demonstrated 17.81% and 531.41% increase in the first-mode frequencies compared to the NACA 2412 and the RCS wing. Moreover, in case of all the modes, the GST wing exhibited the highest frequency. Such variations indicate the significance of wing geometry in determining structural response, particularly when subjected to hydrodynamic loading.

Fig. 4 illustrates the pressure distribution plot for the suction and pressure sides of the wings. In contrast, Fig. 5 represents the velocity contours at the mid-span plane (Z = 0.2m) along with velocity streamlines. In the velocity contour plots of the RCS configuration, the zigzag pattern observed in the suction side as well as the pressure side represents the variation in the span. This variation can be attributed to the separation and reattachment of the boundary layer. The zones of high and low velocities represent the unsteady motion of the fluid layer as it oscillates towards the surface before it forms large-scale vortices in the downstream. The phenomenon signifies transitional shear-layer instability typical of flat, low-camber geometries with sharp leading edges, and explains the onset of the broad, low-frequency wake observed in the velocity field. The suction-side pressure pattern of RCS wing, as illustrated in Fig. 4(i), further demonstrates the weak, distributed suction and spanwise irregularities, indicating that the shear layer is not forced into immediate compact roll-up; instead, it remains thin and unstable, convects, and finally rolls up downstream, producing the long vortex-formation length and the zigzag wake pattern visible in the velocity plots. This delayed roll-up leads to large-scale, low-frequency wake structures and a broadened PSD peak, as illustrated in Fig. 6.

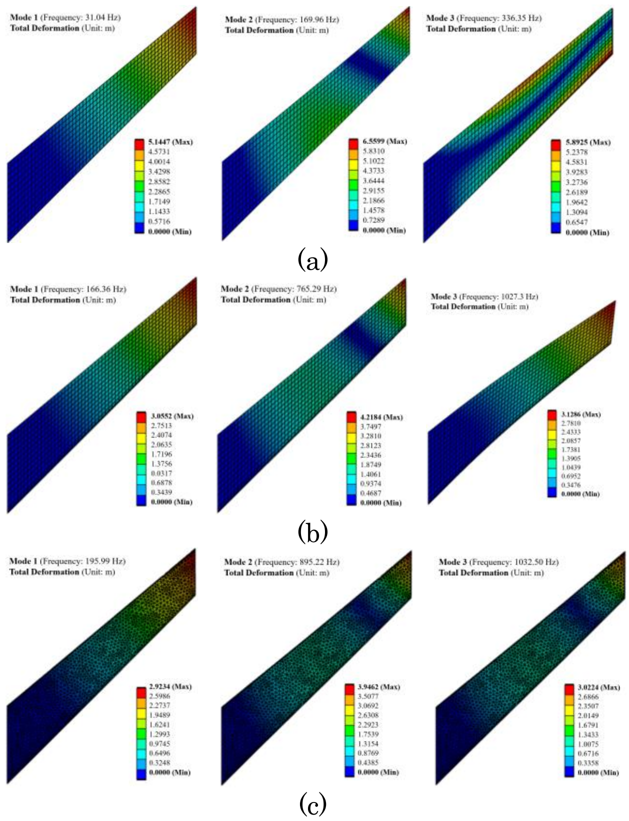

Fig. 3 Three different mode shapes on the wings (a) RCS, (b) NACA 2412, (c) GST, representing modes 1, 2, and 3 from left to right order for each of the wing configurations.

Compared to the RCS wing, the NACA 2412 and GST-inspired wings reveal distinct differences in wake stability, surface pressure distribution, and the resulting vortex-induced vibration (VIV) characteristics. As seen from Fig. 4 (ii), the NACA 2412 wing produces a narrow, attached flow with a thin shear-layer roll-up into compact, repeatable vortices, yielding a smaller characteristic wake width (D).

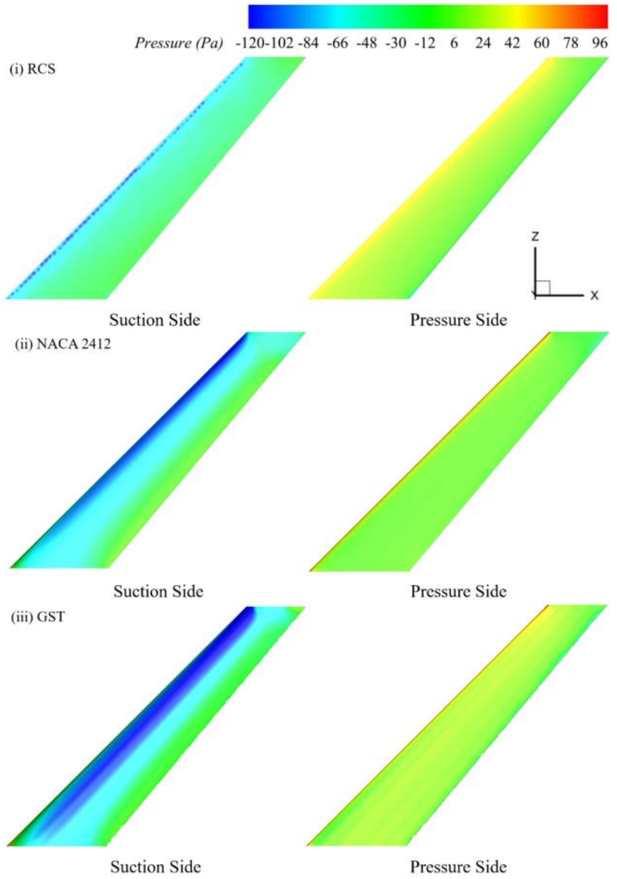

Fig. 4 Pressure contour on suction and pressure surfaces of the considered wing configurations.

According to the Strouhal scaling ($f = St \cdot U/D$, where *St* is the Strouhal number, and U is the free-stream velocity), this smaller wake yields a higher VSF, observed with a peak at 3.36 Hz as shown in Fig. 6. The velocity contours confirm this behavior, showing a thin, high-momentum wake and tightly packed, regularly convecting vortices downstream of the trailing edge, features that produce strong periodic lift fluctuations and a distinct frequency peak in the PSD spectrum. In contrast, the GST-inspired wing exhibits a visibly broader but more diffused wake region with gradual velocity recovery and minimal spanwise asymmetry. The flow separates smoothly and reattaches farther downstream, forming larger but slower-evolving coherent structures. This extended vortex-formation length and weaker shear-layer roll-up reduce the characteristic shedding frequency, as evidenced by the much lower dominant frequency of 0.08 Hz.

The surface pressure distributions further strengthen this interpretation. On the suction side, the NACA 2412 wing exhibits a steep pressure gradient near the leading edge, with localised low-pressure zones indicative of strong suction peaks and fluctuating lift generation. The GST-inspired wing, however, maintains a smoother pressure recovery with a more uniform low-pressure region across the span and weaker gradients on the pressure side, illustrated in Figure 4(iii). This more even pressure distribution indicates suppressed shear-layer instability and reduced instantaneous hydrodynamic loading. Consequently, while the NACA 2412 geometry is dominated by rapid, thin shear-layer roll-up that produces repeatable vortices and a sharp PSD peak, the GST-inspired configuration promotes quasi-steady, large-scale vortex structures with slower temporal evolution, lower unsteady lift amplitude, and diminished spectral sharpness. These combined velocity-pressure features confirm that the GST wing produces more stable wake interactions and lower unsteady force fluctuations, thereby minimising the risk of resonance and improving the long-term hydrodynamic stability of underwater glider wings.

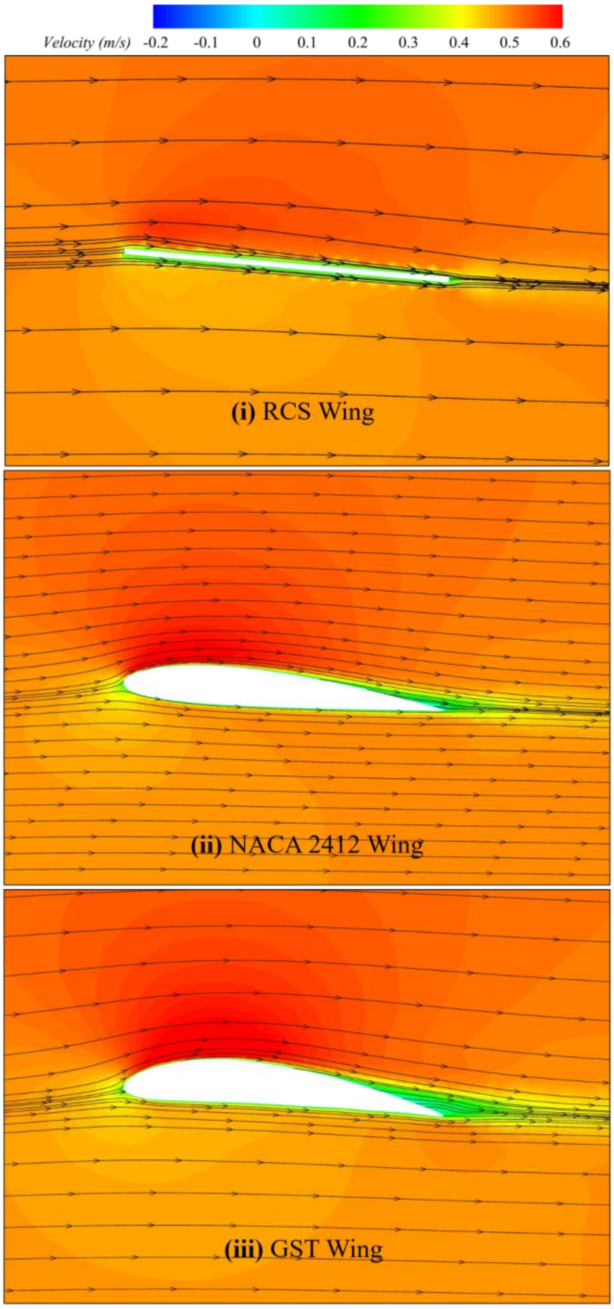

Fig. 5 Velocity contour at Z = 0.2m (at the middle) of the considered wing configurations.

The unsteady lift-force signal obtained from CFD indicates a dominant VSF, which represents the forcing that could induce flow-induced vibrations if the wing were flexible. This frequency was compared to the natural frequencies of the wing to assess the risk of resonance (presented in Fig. 7). For all three wing geometries, the first wet natural frequency (corrected for hydrodynamic added mass using Eq. (1) and (2)) remained significantly higher than the VSFs derived from FFT, especially in case of the NACA 2412 and GST wing.

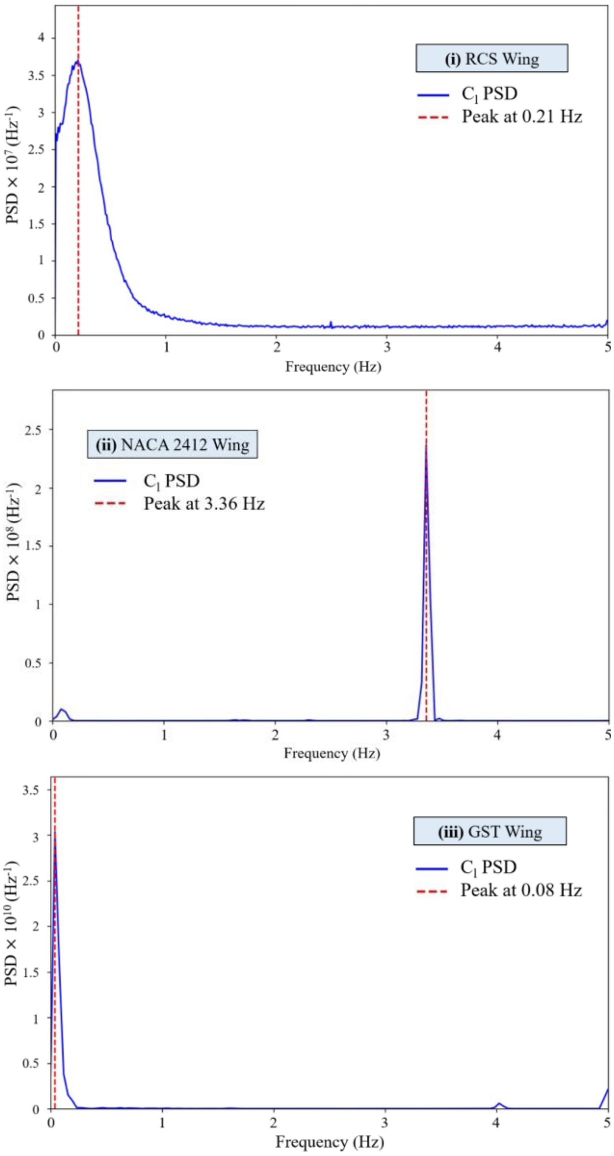

Fig. 6 Power spectral density of the lift coefficient time history of the considered wing configurations.

Accounting for the PSD amplitudes, the RCS wing exhibits the largest absolute unsteady energy (in the order of 10^{-7}), with a broad low-frequency spectral distribution and a peak near 0.21 Hz. This indicates the strongest overall lift fluctuations concentrated at low frequency, caused by large-scale, slowly evolving wake motions from delayed shear-layer roll-up. Although the energy is spectrally broad (low spectral sharpness), the absolute magnitude of unsteady forcing is highest for RCS, which, combined with its low first natural frequency (~28.35 Hz), implies a smaller safety margin (~28.14 Hz) against long-term cyclic loading and a greater susceptibility to cumulative damage. The NACA 2412 wing produces a narrow, moderate-amplitude spectral peak (in the order of 10^{-8}) at 3.36 Hz, indicating coherent and periodic vortex shedding. While its PSD peak magnitude is lower than the amplitude for that of the RCS wing, the concentration of energy into a single frequency band yields strong, repeatable periodic forcing on the structure. NACA 2412 wing's first wet natural frequency (~112.35 Hz) remains far above this VSF by 108.99 Hz, but the structured periodic excitation could still drive moderate cyclic stresses

stiffness increases the likelihood of convergence between VIV and modal frequencies. On the other hand, the GST-inspired wing produces more stable wake interactions and over long deployments. The GST-inspired wing shows the smallest absolute PSD amplitude (in the order of 10^{-10}) with a weak peak at 0.08 Hz, reflecting minimal unsteady lift excitation. The broad and diffused wake, along with uniform surface pressure distribution, produces both lower-frequency and lower-amplitude forcing, which together maximise the gap by 132.33 Hz to the GST's relatively high first wet natural frequency of ~132.41 Hz. Therefore, the GST geometry offers the most favourable dynamic behaviour, the lowest unsteady forcing amplitude, and the largest frequency separation from structural modes, implying the lowest resonance risk under the operational conditions.

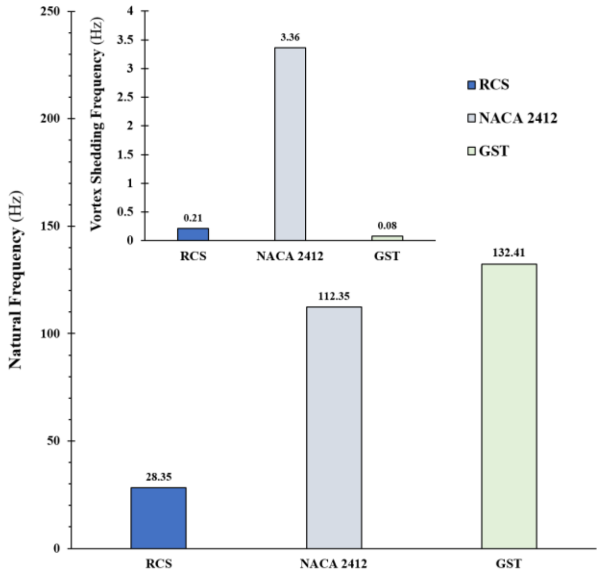

Fig. 7 Comparison between wet natural frequency and VIV frequency for each type of wings.

Additionally, in the study of Wang *et al.* (2025), the authors considered an additional mass (acoustic payload) at the end of the wing, attached at the wingtip [3]. From mode 1 in Fig. 3(a), we also observed that the wing tip is the location of maximum displacement. Adding mass at locations of maximum mode displacement significantly lowers the corresponding natural frequency [10]. Thus, if the considered configurations of this study had an additional mass/payload at the end of the wingtip, similar to Wang *et al.* (2025) [3], the first mode would have been substantially lower than the ones obtained in this study. Such payloads attached at the wingtip of the wings for determining both the natural frequencies and the dominant VSFs would have substantially indicated the increased likelihood of resonance.

4. Conclusion

This study demonstrates that the replacement of conventional flat-plate RCS wings of UWGs with streamlined profiles such as NACA 2412 and GST-inspired shapes has the potential to enhance hydrodynamic stability and reduce the possibility of resonance by maintaining a large separation between vortex shedding and natural frequencies. The RCS wing is not only hydrodynamically less efficient, but also has greater susceptibility towards long-term fatigue on account of the fact that its reduced

lower unsteady force fluctuations, thereby reducing the risk of fatigue. In both NACA 2412 and GST-inspired wing profiles, the natural frequencies are far from VSFs in the considered operating regime, thereby ensuring structural safety. The findings of this study indicate that the incorporation of a baseline as well as a biomimetic airfoil has the positive prospect of reducing the wake instability and resonance risk associated with UWG wings. Moreover, they emphasise the importance of intensive study on the application of other choices of cross-sections for the UWG wing from the wide variety of bio-inspired airfoil libraries. Future work needs to incorporate payload-induced tip mass effects for more accurate resonance predictions and assessment of long-term fatigue performance under realistic mission conditions.

References

[1] Hossain, G.A. *et al.* (2025) "Recent advancements in biomimetic application in underwater glider development: Current opportunities and future trends," *Ain Shams Engineering Journal*, 16(7), p. 103410.

[2] Hossain, G.A. *et al.* (2024) "Design Modification of Slocum Underwater Glider: A Numerical Approach," in *9th BSME International Conference on Thermal Engineering (BSME ICTE 2024)*. Dhaka: Bangladesh Society of Mechanical Engineers.

[3] Wang, Y. *et al.* (2025) "Study on the generation mechanisms of hydrodynamic noise in underwater glider wings based on bidirectional fluid–structure interaction," *Physics of Fluids*, 37(8).

[4] Masud, M.H. and Dabnichki, P. (2023) "Feasibility of penguin geometric features for the biomimetics applications: overview and analysis," *Meccanica*, 58(5), pp. 847–858.

[5] van der Geest, N. *et al.* (2022) "New insight into the swimming kinematics of wild Green sea turtles (*Chelonia mydas*)," *Scientific Reports*, 12(1), p. 18151.

[6] van der Geest, N. *et al.* (2023) "New Insights into Sea Turtle Propulsion and Their Cost of Transport Point to a Potential New Generation of High-Efficient Underwater Drones for Ocean Exploration," *Journal of Marine Science and Engineering*, 11(10), p. 1944.

[7] Williamson, C.H.K. and Govardhan, R. (2004) "Vortex-induced vibrations," *Annual Review of Fluid Mechanics*, 36(1), pp. 413–455.

[8] Mittal, R. and Balachandar, S. (1995) "Effect of three-dimensionality on the lift and drag of nominally two-dimensional cylinders," *Physics of Fluids*, 7(8), pp. 1841–1865.

[9] Bearman, P.W. (1984) "Vortex Shedding from Oscillating Bluff Bodies," *Annual Review of Fluid Mechanics*, 16(1), pp. 195–222.

[10] Newman, J.N. (2018) *Marine hydrodynamics*. The MIT Press.

[11] Sarpkaya, T. (2003) *A critical review of the intrinsic nature of vortex-induced vibrations*. Monterey, California.

[12] Sarpkaya, T. (2004) "A critical review of the intrinsic nature of vortex-induced vibrations," *Journal of Fluids and Structures*, 19(4), pp. 389–447.

[13] Kaminski, A. and McDaniel, J.G. (2024) "Natural Frequency Perturbations Using a Scalar Expression with Reference Plots to Predict Associated Errors," *Journal of Vibration Engineering & Technologies*, 12(1), pp. 719–736.